ACS OMEGA

http://pubs.acs.org/journal/acsodf

Article

Molecular Recognition of Glycan-Bearing Glycomacromolecules Presented at Membrane Surfaces by Lectins: An NMR View

Marta G. Lete,[▽] Miriam Hoffmann,[▽] Nils Schomann, Ane Martínez-Castillo, Francesca Peccati, Patrick B. Konietzny, Sandra Delgado, Nicole L. Snyder, Gonzalo Jiménez-Oses, Nicola G. A. Abrescia, Ana Ardá, Laura Hartmann,* and Jesús Jiménez-Barbero*

Cite This: *ACS Omega* 2023, 8, 16883−16895

Read Online

ACCESS | Metrics & More | Article Recommendations | Supporting Information

ABSTRACT: Lectin−glycan interactions are at the heart of a multitude of biological events. Glycans are usually presented in a multivalent manner on the cell surface as part of the so-called glycocalyx, where they interact with other entities. This multivalent presentation allows us to overcome the typical low affinities found for individual glycan−lectin interactions. Indeed, the presentation of glycans may drastically impact their binding by lectins, highly affecting the corresponding binding affinity and even selectivity. In this context, we herein present the study of the interaction of a variety of homo- and heteromultivalent lactose-functionalized glycomacromolecules and their lipid conjugates with two human galectins. We have employed as ligands the glycomacromolecules, as well as liposomes decorated with those structures, to evaluate their interactions in a cell-mimicking environment. Key details of the interaction have been unravelled by NMR experiments, both from the ligand and receptor perspectives, complemented by cryo-electron microscopy methods and molecular dynamics simulations.

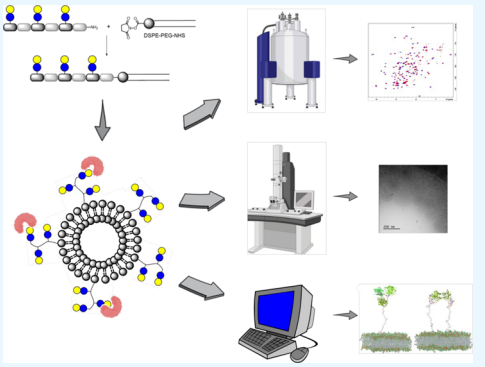

1. INTRODUCTION

Lectins, carbohydrate-recognizing proteins, are ubiquitous in nature, present in microorganisms, plants, and animals. Within the cell, they can be found in different locations, including the nucleus, plasma membrane, or cytosol.[1] One important family of lectins are the galectins (Gal), which bind β-galactoside-terminated glycans and are involved in a myriad of biological processes including cell migration, inflammation, autophagy, or immune response.[2] Indeed, dysregulation of galectins has been linked to severe diseases, such as cancer,[3] fibrosis, or cardiovascular pathologies.[4] Although initially it was thought that they only recognized endogenous glycans, it was later observed that galectins are also able to bind exogenous ligands present at the surface of a variety of entities, such as bacteria, parasites, or fungi, linking them to the innate immune system.[5,6]

In general, lectin−glycan interactions display low affinity, in the millimolar to micromolar range. To achieve stronger binding required for biological interactions, nature often employs the multivalent presentation of glycans.[7] This is most commonly realized through the multivalent presentation of multiple glycans on the cell surface as part of the so-called glycocalyx, where they are presented to lectins in different glycoconjugate forms, such as glycoproteins, glycolipids, or proteoglycans.[8] The type of presentation of glycans is known to critically impact their recognition by lectins and may drastically affect the corresponding binding affinity and even selectivity.[9,10] Moreover, glycan recognition of the glycocalyx is affected by processes such as membrane diffusion and crowding events of glycans, and the dynamic features of these interactions are an aspect that should be highlighted in the study of these interactions.[11,12] Herein, we have chosen galectins as the model system. In the case of galectins in particular, multivalent processes on the cell surface contribute greatly to their biological activity as they can oligomerize in the presence of multivalent ligands and also induce cross-linking of glycoconjugates, leading to the formation of galectin lattices.[13,14] Such lattices are known to regulate processes such as cell binding and migration, cellular trafficking, and signal transduction.[13,14] Therefore, the use of membrane-bound glycans and membrane-based systems is of great importance in the study of galectin−ligand interactions.

To address galectins with suitable ligands, the use of multivalent natural and synthetic glycan structures mimicking natural glycans and glycan conjugates is a well-known approach. Indeed, diverse investigations[15−20] have shown that the avidity of glycan−protein interactions can be

Received: January 31, 2023
Accepted: April 18, 2023
Published: May 3, 2023

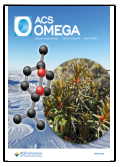

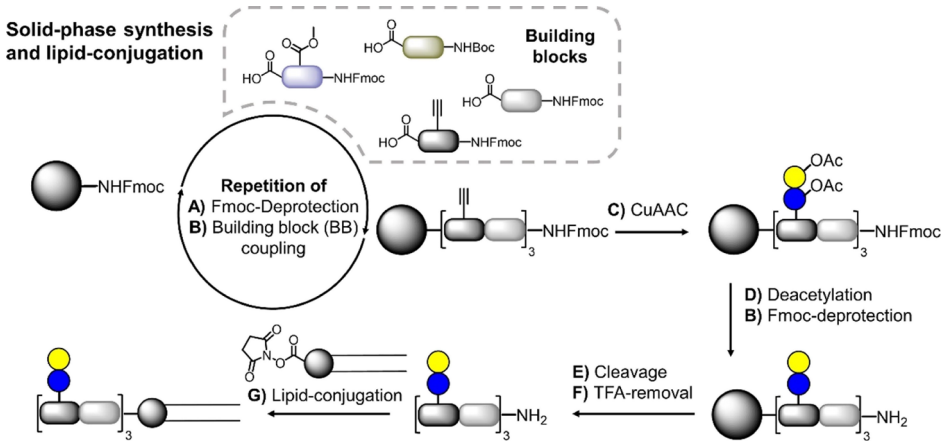

Figure 1. (A) 25% Piperidine in DMF, 10 min + 20 min. (B) BB (5 equiv), PyBOP (5 equiv), DIPEA (20 equiv) DMF, 1 h. (C) Lactose azide (2.5 equiv per alkyne), $CuSO_4$ (50 mol % per alkyne), NaAsc (50 mol % per alkyne), DMF/water, overnight. (D) NaOMe, MeOH, 2 × 30 min h. (E) 95% TFA, 2.5% TIPS, and 2.5% DCM, 1 h. (F) Anion exchange resin, 1 h. (G) For **L1** and **L6**: **1** or **6** (8 equiv), DSPE-PEG-NHS (1 equiv), $NaHCO_3$-buffer/DMF (9/1), overnight, dialysis; for **L2** to **L5**: **2**, **3**, **4**, or **5** (5 equiv), DSPE-PEG-NHS (1 equiv), DIPEA (20 equiv), DMSO, overnight, dialysis; for compounds with MDS as BB (not shown in this figure), the following additional reaction conditions were applied: 0.2 M LiOH THF/water (1/1), 2 × 1 h; and HATU (3 equiv), DIPEA (10 equiv), 4-amino benzene sulfonic acid (3 equiv), DMF, 1.5 h; for further details see Materials and Methods and the Supporting Information.

significantly increased in vitro through multivalent presentation also on non-natural scaffolds such as polymers or in synthetic membranes such as liposomes.[21] The chemical diversity of biocompatible materials to realize multivalent glycan presentation and to monitor lectin−glycan interactions is massive (organic molecules, glycopeptides, cyclodextrins, self-assembling polymer clusters, dendrimers, gels, micelles, etc.).[22] Nevertheless, as stated above, mimicking the natural presentation involves designs that need to be carefully verified since the parameters such as glycan density and mode of presentation affect the molecular recognition event, both in vitro and in vivo.[23] Other key structural parameters are the scaffold and linkers to which the glycans are attached and the platform employed for the decoration.[24] Furthermore, liposomes are recognized in this context to not only provide multivalent presentation but also function as cell mimetic systems[25,26] since the properties and dynamics provided by the lipids forming the artificial bilayer resemble the in vivo natural membrane.

Previous studies by the authors described the synthesis of lactose-functionalized oligo(amidoamines) as highly defined, synthetic, multivalent glycomacromolecules to target galectins. They showed that through introduction of secondary non-glycan-binding motifs, heteromultivalent glycomacromolecules are accessible, which efficiently bind to human galectin-3 (hGal3) under different experimental conditions. It was deduced that the affinity was notably increased by the introduction of additional non-saccharide functionalities on the oligo(amidoamine) backbone versus the solely lactose-functionalized structures (high μM).[27] Furthermore, presentation of homomultivalent ligands on liposomes was shown to increase the overall avidity of the system toward hGal3.[28] However, the actual features of the improved interactions were not evident, especially from the structural and dynamical perspectives.

In this context, we herein present the study of the interaction of a variety of homo- and heteromultivalent lactose-functionalized glycomacromolecules, presented individually or embedded into liposomes, with two human galectins, the carbohydrate recognition domain of human hGal3-CRD, a monomer, and human Gal1 (hGal1), a homodimer. Key details of their dynamic properties and their interactions in solution and in a cell-mimicking environment (liposomes) have been revealed by NMR experiments,[29] both from the ligand [saturation-transfer difference (STD)-NMR] and receptor perspectives [^{1}H−^{15}N heteronuclear single quantum coherence spectroscopy (HSQC), including competition experiments), complemented by cryo-electron microscopy (cryo-EM) methods and molecular dynamics (MD) simulations to assess the formation of specific complexes and the generation of macromolecular assemblies.

2. RESULTS AND DISCUSSION

2.1. Synthesis of Homo- and Heteromultivalent Glycomacromolecules and Their Lipid Conjugates.

Galectins (hGal1 and hGal3-CRD) recognize lactose moieties;[30,31] however, they only do so with low micromolar affinity. Typically, two strategies are employed to increase affinity: multivalent presentation or the introduction of secondary, non-glycan-binding motifs. In a previous study, we demonstrated that the combination of both lactose and sulfonate-substituted aromatic residues in a multivalent fashion leads to an apparent increase in binding to Gal3.[27] Based on these results, we selected mono- and trivalent lactose-bearing glycomacromolecules with and without benzene sulfonic acid as target ligands as well as different control structures, e.g., the macromolecular scaffold itself and monovalent presentation of the sulfonate. All glycomacromolecules were synthesized via previously established solid-phase polymer synthesis protocols as illustrated in Figure 1.[32−34] In short, building blocks carrying a free carboxylic acid group and an Fmoc-protected amine functionality were coupled to an amine-functionalized resin using PyBOP and *N*,*N*-diisopropylethylamine (DIPEA) as coupling agents. Following the coupling step, Fmoc-deprotection was conducted with piperidine to release a free amine at the *N*-terminus to which another building block was then coupled. Repeating this stepwise procedure, a monodisperse, sequence-controlled oligo(amidoamine) scaffold was assembled.

https://doi.org/10.1021/acsomega.3c00634
ACS Omega 2023, 8, 16883−16895

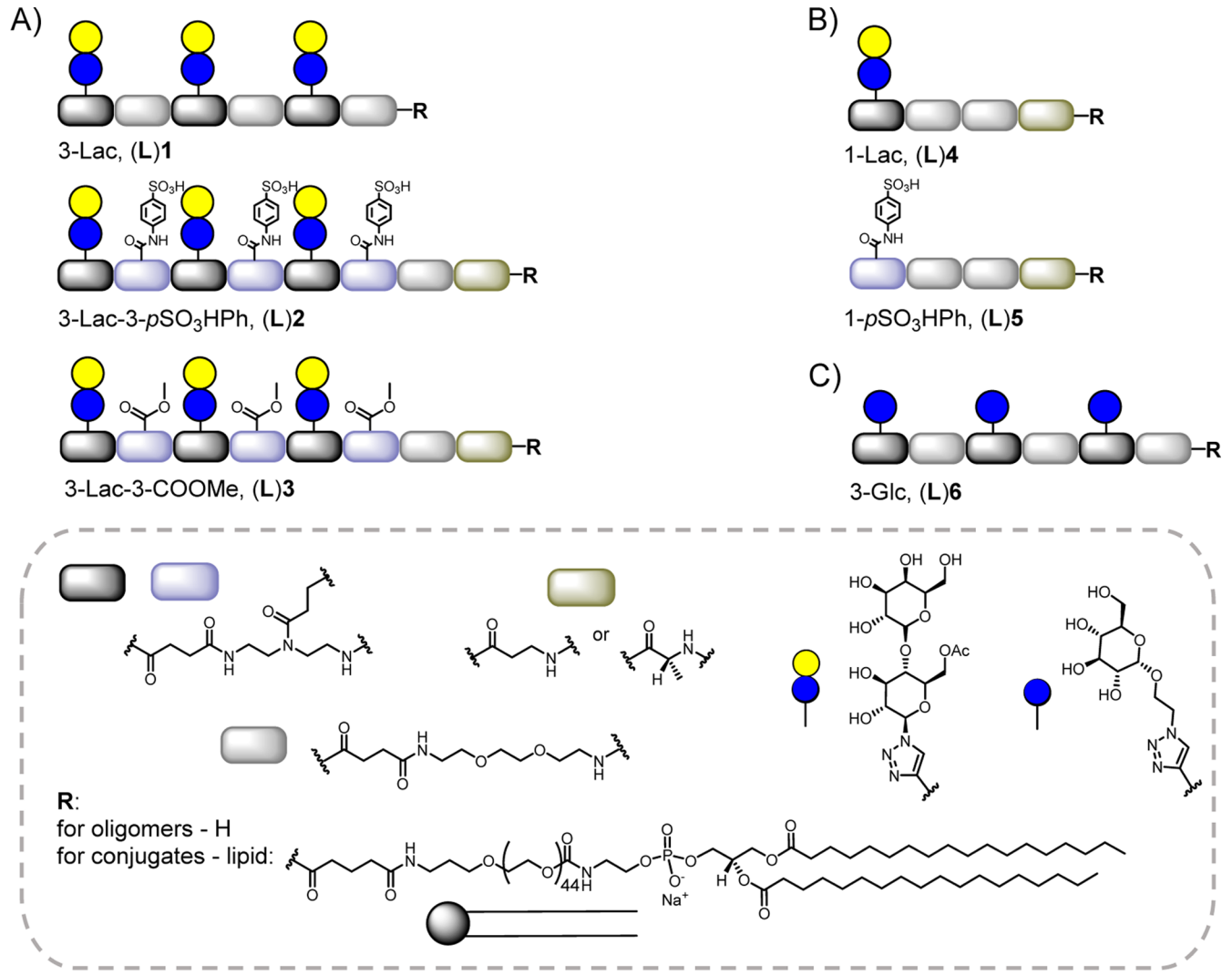

Figure 2. Overview of the synthesized glycomacromolecules (R = H) and the respective lipid conjugates (R = DSPE-PEG-lipid, marked with **L**): (A) trivalent lactose-functionalized compounds [(**L**)**1**−**3**], with **2** carrying additional *p*-amino benzene sulfonic acid residues and **3** bearing the respective protected carboxylic acid side chains of the MDS building block. (B) Monovalent lactose-((**L**)**4**)- or *p*-amino benzene sulfonic acid-((**L**)**5**)-functionalized structures. (C) Glc-functionalized control structure (**L**)**6**.

Here, triple bond diethylenetriamine succinyl, 1-(fluorenyl)-3,11-dioxo-7-(pent-4-ynoyl)-2-oxa-4,7,10-triazatetra-decan-14-oic acid (TDS)[32] was used as a alkyne-functionalized building block to enable subsequent conjugation of azide-carrying carbohydrate ligands to sidechains of the backbone via copper(I)-catalyzed alkyne−azide cycloaddition (CuAAC). Methyl succinyl diethylenetriamine succinyl, 1-(9*H*-fluoren-9-yl)-7-(4-methoxy-4-oxobutanoyl)-3,11-dioxo-2-oxa-4,7,10-triazatetradecan-14-oic acid (MDS)[27] carrying a protected carboxylic acid side chain functionality was used to allow for orthogonal amide coupling of 4-amino benzene sulfonic acid, thereby enabling the synthesis of heteromultivalent ligands. Finally, ethylene glycol diamine succinyl, 1-(9*H*-fluoren-9-yl)-3,14-dioxo-2,7,10-trioxa-4,13-diazaheptadecan-17-oic acid (EDS)[35] was used as a spacer introducing an ethylene glycol motif in the main chain. By using different combinations of the chosen building blocks, the targeted set of glycomacromolecules was synthesized (Figure 2): The trivalent lactose-functionalized glycomacromolecule **1** and for comparison, the monovalent compound **4** were synthesized by alternating TDS and EDS. The heteromultivalent compound **2** was obtained by exchanging EDS in **1** against MDS and orthogonal coupling of 4-amino benzene sulfonic acid via amide formation and azido-lactose via CuAAC to the MDS and TDS side chains, respectively. As reference, the same scaffold was synthesized and functionalized with lactose, but leaving the carboxylic acid carrying side chains of MDS protected. Further control structures were derived, with **5** carrying only the 4-amino benzene sulfonic acid-residue and the trivalent structure **6** functionalized with glucose (Glc) as the non-binding partner for galectins.

After scaffold assembly and functionalization, the molecules were de-*O*-acetylated under Zemplén conditions.[36] Finally, the glycomacromolecules were obtained after acidic cleavage and purification with an anion-exchange resin and preparative reversed phase high-performance liquid chromatography (RP-HPLC) with high purity (see the Supporting Information for details of the synthesis and analytical data). All structures were characterized via ^{1}H-NMR-analysis, HR-MS, and RP-HPLC-MS. With the exception of structures **2** and **4**, relative purities ≥ 95% were determined via integration of the UV-signal of the RP-HPLC chromatogram at λ = 214 nm. Due to its polar

https://doi.org/10.1021/acsomega.3c00634
ACS Omega 2023, 8, 16883−16895

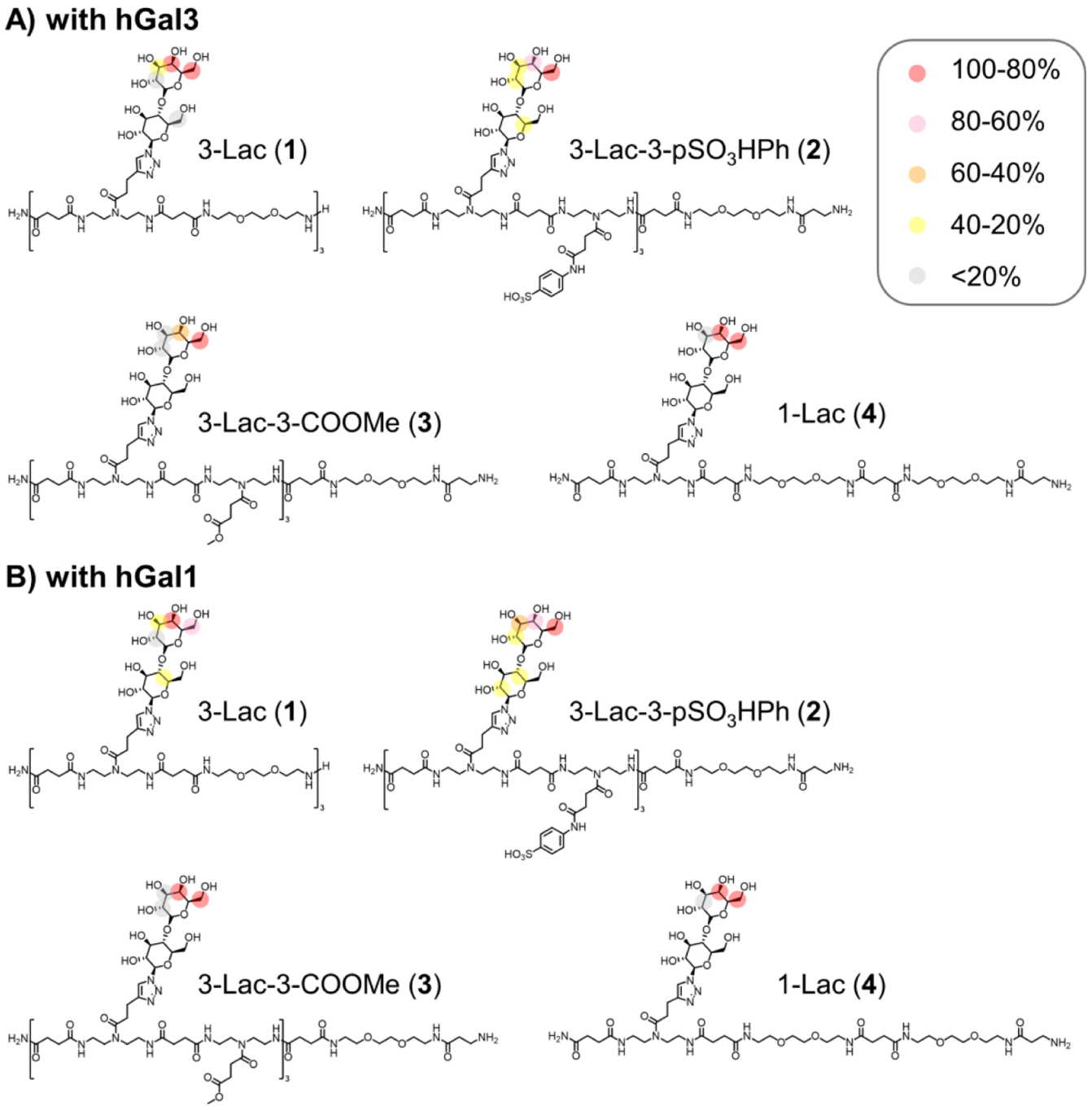

Figure 3. ^{1}H-STD-NMR epitope map for the interaction of (A) hGal3 (40 μM) with glycomacromolecules **1**, **2**, **3** (8:1 molar ratio), and **4** (30:1 molar ratio). (B) ^{1}H-STD-NMR epitope map for the interaction of hGal1 with the glycomacromolecules under analogous experimental conditions. The on-resonance frequency was set at the aliphatic region (~0.80 ppm) and the off-resonance frequency at −25 ppm.

properties, **2** elutes with the injection peak; however, the high resolution of NMR data and mass spectrometry allow one to assume high purity of this compound as well. With respect to **4**, a mixture of the target structure and a deletion sequence with one missing *p*-amino benzene sulfonic acid residue was detected and could not be separated by chromatography. Target structure and deletion sequence together provide again a relative purity of 95%. We decided to continue our study with this two-component mixture as we can still conclude on the effects of introducing the secondary binding motifs (independent of whether it is exactly two or three per glycomacromolecule) in binding to the galectin CRD as analyzed by STD-NMR and for comparison to the homomultivalent glycomacromolecules.

The nomenclature of the structures used in the following discussion (Figure 2) describes the main features of the compounds: Compound **1**, for example, is named 3-Lac as it is a trivalent lactose-functionalized glycomacromolecule. In contrast, structure **2** is called 3-Lac-3-*p*SO_3HPh, indicating the functionalization of the backbone with three lactose- and three *p*-amino benzene sulfonic acid residues.

Lipid conjugation was then conducted according to previously published protocols to obtain glycoconjugates **L1** and **L6** (see the last step in Figure 1).[37] In particular,

https://doi.org/10.1021/acsomega.3c00634
ACS Omega 2023, 8, 16883−16895

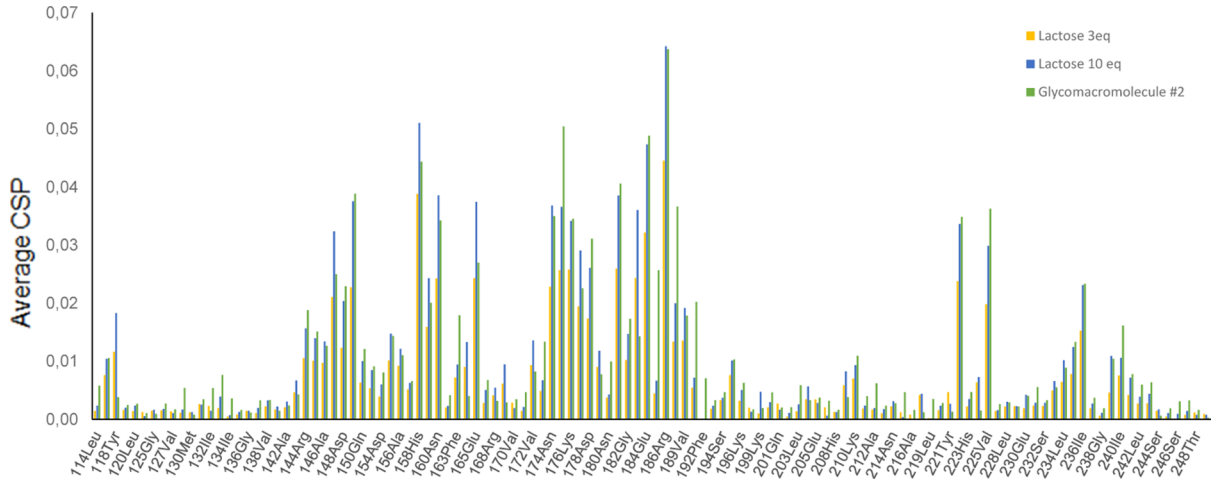

Figure 4. (A) CSP measured for the backbone amides of hGal3-CRD upon binding to **2** (1:1 ratio) compared to those obtained in the presence of 3 and 10 equiv of free lactose.

commercially available lipid DSPE-PEG-NHS in a mixture of DMF and $NaHCO_3$ (aq.) (1/10) was conjugated to the free amines of **1** and **6** overnight. For **L2** to **L5**, the reaction conditions were slightly varied, using now DMSO as a solvent and DIPEA as a base. It should be noted that conjugation of molecules of such different polarities and amphiphilic properties is challenging. In particular, solvent selection, purification, and the tendency of the NHS-ester of the lipids to hydrolyze over time can prevent full conversion and reduce yields.[38] The latter is also supported by the MALDI-TOF-MS data which show the hydrolysis product of the lipid. All lipid−glycomacromolecule conjugates (Figure 2) were purified via dialysis with a high molecular weight cut-off of 7000 Da that should provide for complete removal of excess glycomacromolecules, still retaining free lipid and the lipid conjugates in the dialysis device.[37] After freeze-drying the lipid/lipid-conjugate mixtures were characterized by ^{1}H-NMR spectroscopy and MALDI-TOF-MS. For **L1**, **L3**, and **L6**, where the molecular weight of the glycomacromolecule used in the conjugation is within the MALDI-TOF-MS detection range, MALDI-TOF-MS data of the conjugates after dialysis confirms that no signals for the free glycomacromolecules were detected (see the Supporting Information), except for **L2**, for which no decent MALDI-TOF-MS data could be achieved. ^{1}H-NMR analysis was used to determine the conversion according to previously published work (see the Supporting Information for further details on the synthesis and analytical data).[28] The obtained conversion was further used in the calculation of the liposomal formulation to obtain comparable amounts of ligands.

2.2. Binding of Galectins to Homo- and Hetero-multivalent Glycomacromolecules. *2.2.1. Ligand's Perspective.* First, the binding features of both galectins (hGal3 and hGal1) to the free glycomacromolecules were studied. Both galectins display similar affinity for lactose in the medium micromolar range.[39,40] The binding epitope of the different lactose-containing glycomacromolecules (**1**−**6**) was deduced for hGal3 and hGal1 by employing ligand-based NMR experiments, namely, ^{1}H-STD-NMR.[41,42] Both galectins exclusively bind the lactose moiety of all the constructs.[43] In particular, large STD-NMR intensities were observed for galactose H4, H5, and H6 (Figure 3A). Thus, presentation of the lactose on the macromolecular scaffold does not impede the recognition of the lactose itself or accessibility to the galectin-binding sites. No other regions of the constructs seem to contribute significantly to the binding event. Surprisingly, also the sulfonate residues in glycomacromolecule 3-Lac-3-*p*SO_3HPh (**2**) did not affect the STD-NMR response (see Supporting Information Fig. S2).

2.2.2. Lectin's Perspective. In the next step, the interaction with the free ligand in solution was studied from the viewpoint of the protein using ^{15}N-labeled hGal3-CRD and the trivalent glycomacromolecule 3-Lac-3 *p*SO_3HPh (**2**) as models via ^{1}H−^{15}N 2D HSQC NMR, and the corresponding chemical shift perturbations (CSPs) of the cross peaks were measured. With these experiments, the lectin residues that are involved in the interaction with the sugar moiety of the glycomacromolecule can be distinguished.[43] Generally speaking, CSP are used to obtain structural information on the molecular recognition event since the intrinsic chemical shifts of the amide signals of the protein are strongly influenced by the interaction with the ligand: the chemical environment at the lectin's binding site is modified by the presence of the ligand. First, we compared the CSP of hGal-3 to free lactose to the CSP of the protein binding the multivalent glycomacromolecules in separate experiments. From the observed experimental CSP for the mixture of hGal3-CRD and 3-Lac-3-*p*SO_3HPh (**2**) in a 1:1 ratio to those obtained in the presence of different equivalents of free lactose (Figure 4), it was deduced that the observed CSP in the presence of 1 equiv of **2** (which corresponds to 3 equiv of lactose) is similar to those measured in the presence 10 equiv of free lactose. Possibly, the observed enhancement of the interaction is due to the multivalent presentation which enables multivalent processes such as statistical rebinding.[44] The results also support the findings of the STD-NMR experiments as only the regions of the protein are perturbed in the interaction with the heteromultivalent glycomacromolecule, which are also affected by binding lactose. No other parts of the protein were found to participate in the interaction.

In contrast, for hGal1, a different phenomenon took place. A dramatic reduction in the intensity of many hGal1 HSQC cross peaks was observed (see Supporting Information, Figure S3), strongly suggesting that the free-bound exchange process associated to the interaction event takes place in the intermediate range of the chemical shift time scale and that, therefore, the associated binding affinity is stronger. The

https://doi.org/10.1021/acsomega.3c00634
ACS Omega 2023, 8, 16883−16895

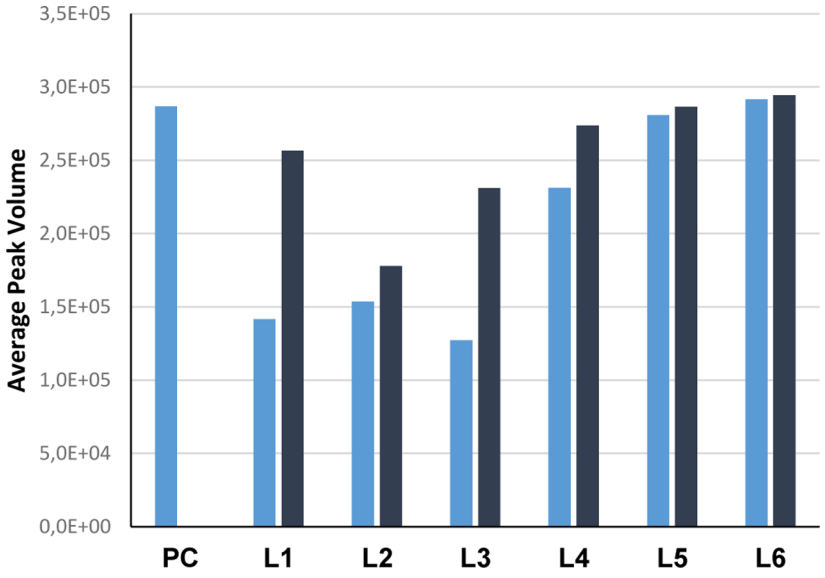

Figure 5. Quantification of the peak volume reduction of hGal3 CRD upon binding to liposome-containing glycomacromolecules (light blue bars) and subsequent intensity recovery by the addition of 20 equiv of lactose (dark blue bars). As control, the first bar, where the light blue bar is the intensity of the protein in the presence of naked liposomes (PC only).

presence of high-order complexes given the presence of two lactose binding sites in hGal1 can be hypothesized. In fact, cross-linking events may take place for the multivalent ligand interacting with the dimeric hGal1. This evidence is further supported by the observation of precipitation in the NMR sample.

2.3. Multivalent Glycan−Galectin Interactions in a Model Membrane. Subsequently, the multivalent glycomacromolecules functionalized with a phospholipid were embedded into model lipid bilayers to try mimicking the natural multivalent presentation that takes place in the cell. In particular, they were mixed with eggPC (L-α-phosphatidylcholine) to generate liposomes.

Ligand-based NMR experiments, such as STD-NMR, are of paramount importance to monitor ligand−receptor interactions when the ligands are small and tumble fast in solution, in the picosecond time scale. Given the large size of the glycomacromolecule-functionalized liposomes, these type of NMR methods were not attempted and only receptor-based NMR methods using the ^{15}N-labeled galectins were employed to monitor the interaction between the sugars displayed at the liposomes and the soluble galectins. It was hypothesized that the interaction of the galectin with the liposome-containing glycopolymer would heavily affect some NMR parameters of the NMR active nuclei of the lectin. In particular, the decrease of signal intensities of the ^{1}H−^{15}N 2D HSQC NMR cross peaks of the galectins in the absence and presence of the glycomacromolecule-functionalized liposomes was measured. This phenomenon occurs because, upon binding to the glycan, the effective rotational correlation time of the bound lectin becomes very large, and the associated transverse relaxation rates of their NMR-active nuclei are now fast. Under these conditions, the NMR cross peaks of the N−H amides of the lectin are extensively broadened, and their corresponding cross-peak intensities decrease. The protocol consisted in adding 50 μM of ^{15}N-labeled hGal3-CRD (or hGal1, in separate experiments) to a solution of liposomes containing the glycomacromolecules, followed by recording the NMR spectra. Indeed, CSP accompanied by dramatic intensity losses in the galectin NMR signals were observed only when the lactose-containing glycomacromolecules were present, thus characterizing effective binding (Figure S3 in the Supporting Information). In contrast, when 3-Glc-glycoconjugate (**L6**) or the sugar-lacking 1-*p*SO_3HPh-conjugate (**L5**) were used as controls, neither CSP nor intensity changes were observed. Therefore, all binding events are lactose-mediated and specific. For the monomeric hGal3-CRD, ca. 50% of the cross-peak intensities were lost upon binding to the multivalent glycomacromolecules. A smaller decrease was observed with the monovalent 1-Lac-conjugate (**L4**) (Figure 5). Subsequently, to further prove that the observations are due to specific glycan binding, competition experiments were carried out by adding an excess of lactose (20 equiv) to the NMR tube containing the galectin and the glycomacromolecule−lipid conjugate embedded in the liposome. Since lactose is the canonical ligand for galectins, it was expected that it would effectively compete with the glycan-containing liposomes. The larger the amount of added lactose equivalents required for recovering a given percentage of the initial intensities, the better the affinity of the glycomacromolecule-liposome entity. Fittingly, the addition of 20 equiv of lactose led to effective competition with the liposome−lectin interaction and almost full recovery of the initial HSQC cross peak intensities was observed, except for 3-Lac-3-*p*SO_3HPh-conjugate (**L2**), for which only ca. 70% of the initial intensities were recovered. For 3-Lac-3-COOMe (**L3**), the recovery reached up to 90%. Thus, the analysis of these experiments strongly suggests that **L2** is the best ligand for the CRD of hGal3. This is in agreement with the results obtained in previous studies where the introduction of secondary motifs enhanced the avidity of the glycomacromolecules toward hGal3.[27] Although no direct experimental evidence of the interaction of the lectin with the *p*-amino benzene sulfonic acid residues of 3-Lac-3-*p*SO_3HPh (**2**) could be deduced from the STD-NMR results for the interaction with **2**, the involvement of the SO_3 group in the binding event cannot be discarded. A charge−charge interaction could place the aromatic protons of the ligand far enough from the lectin to generate a negligible STD.

https://doi.org/10.1021/acsomega.3c00634
ACS Omega 2023, 8, 16883−16895

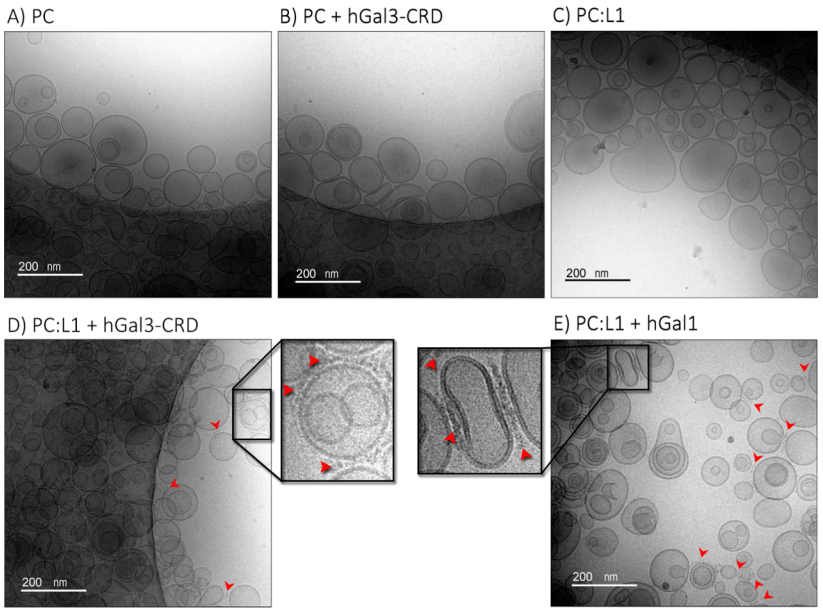

Figure 6. Cryo-EM images. (A−C) Control conditions. (D,E) Liposomes containing 3-Lac-conjugate (**L1**) glycomacromolecules and galectins, which accumulate between membranes (red arrowheads); insets clearly show biological material juxtaposed to the outer leaflet of the liposome membrane.

Scheme 1. Representation of hGal1 Binding in trans or cis Mode to Disaccharide Moieties

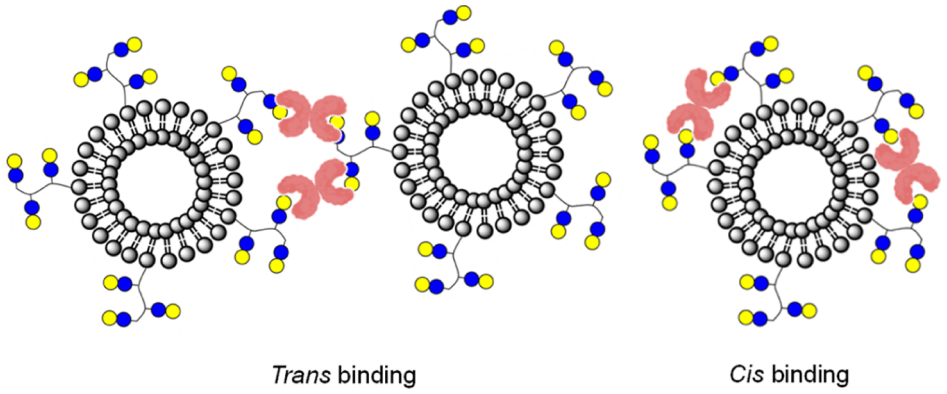

Alternatively, although merely speculative, the conformation/presentation of the glycomacromolecules in solution could be influenced by the aromatic residues, which could establish $\pi-\pi$ interactions and/or anion$-\pi$ interactions.[45] The coil conformation and solvation pattern that can be assumed for the glycomacromolecules based on their scaffold composition and previous studies[46] could be affected by the presence of the charged aromatic residues potentially leading to a different conformation, providing a better accessibility of the lactose units for binding to the lectin. However, no experimental demonstration could be presented.

The same experiments were carried out for homodimeric hGal1 following the same protocol. In this case, all the backbone amide signals were erased from the corresponding 2D HSQC when the liposomes contained not only the trivalent glycomacromolecules (**L1**, **L2** or **L3**) but also monovalent 1-Lac-conjugate (**L4**). Fittingly, as with hGal3-CRD, no interaction was observed with 1-*p*SO_3HPh (**L5**) or 3-Glc (**L6**) (Figure S4 in the Supporting Information). Furthermore, the addition of 20 equiv of lactose was not able to recover the crosspeak intensities at all. This fact highlights the dramatic increase in the strength of the interaction of a dimeric galectin when encountering a multivalent glycan presentation.

This fact strongly suggests that binding of the dimeric hGal1 to the glycomacromolecules embedded into liposomes generates large supramolecular entities, which are invisible to NMR. The use of the monomer hGal3-CRD as a proof of concept has allowed one to study the interaction with the glycomacromolecules in certain detail at the structural level by NMR. However, it is evident that the NMR is not the best technique to employ to obtain detailed information on supramolecular assemblies. Thus, as a further step, binding events taking place at the liposome preparations were monitored by visualizing the samples using cryo-EM. Samples were vitrified for 2D cryo-imaging (see Materials and Methods for further details).

Figure 6(A−C) shows the controls for the liposomes alone in the presence of hGal3-CRD and with the 3-Lac-conjugate (**L1**) incorporated, respectively. Inspection of the obtained images allows one to deduce that the liposomes do not display major contacts among them and behave in an independent manner. In contrast, when the liposomes are decorated with 3-Lac-conjugate (**L1**) and galectins are added, electrodense areas

https://doi.org/10.1021/acsomega.3c00634
ACS Omega 2023, 8, 16883−16895

were clearly observed in between the membranes (marked with red arrowheads), especially when hGal1 was employed.[47] It is tempting to guess that the electrodense areas observed correspond to hGal1 dimers that are crosslinking the lactose moieties in the 3-Lac (**L1**) molecules. The interactions may take place in cis, within the same liposome (Scheme 1), or alternatively in trans mode, connecting disaccharide moieties present at different liposomes. Accordingly, for the experiment with hGal3-CRD, simultaneous binding of several hGal3-CRDs to the same ligand might provide an explanation to the experimental observations, which show much less electrodense areas.

2.4. MD Simulations. To provide further insight into the recognition process and to assess the plausibility of the previously proposed binding modes, 3-Lac-PEG-DSPE glycolipids (**L1**) embedded in a small POPC bilayer in aqueous solution and bound to galectins were modeled through full-atom MD simulations (see Computational Methods) in different ways: one hGal3-CRD molecule binding to each of the lactose units in **L1** (3:1 binding, Figure 7A) and one hGal1 homodimer bound to the external and middle lactose units of two distinct **L1** molecules (2:2 binding, Figure 7B). Both of these situations would nicely explain the occurrence of electrodense areas as observed in the cryo-EM experiments. Interestingly, the PEG chain in the glycolipid was contracted during the simulations due to its large flexibility and the hydrophobic effect, but it was still long enough to maintain the bound lectins away from the membrane throughout the whole simulation time (100 ns). Of note, all lectins remained bound to **L1** in their canonical binding modes observed in related crystallographic structures[48,49] during the simulations, as reflected by the highly conserved geometrical parameters of the bound lactose-units measured along the simulations (Figures S7 and S8 in the Supporting Information). These modeling studies demonstrate the ability of glycolipid **L1** to efficiently and multivalently bind galectins when embedded in liposomes.

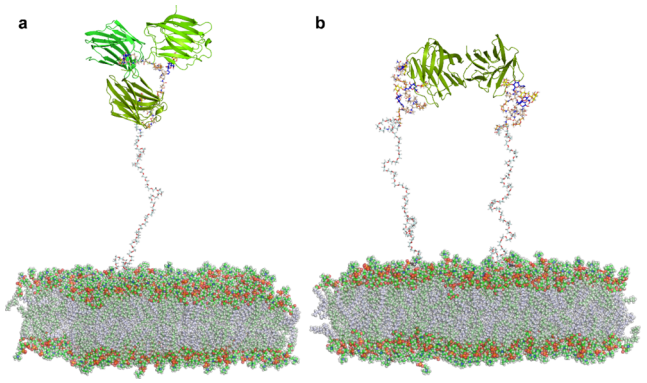

Figure 7. Models of **L1** glycolipids embedded in a POPC bilayer and bound to (a) three hGal3-CRD molecules (3:1 binding) and (b) one hGal1 homodimer (2:2 binding). Each model corresponds to a representative snapshot of a 100 ns MD simulation in aqueous solution (water not shown for clarity).

3. CONCLUSIONS

The synergic combination of NMR data, cryo-EM experiments, and molecular modeling protocols has allowed us to provide a structural view of the molecular recognition events that take place when liposomes decorated with glycan entities interact with their lectin partners. Although the data obtained by using the different experiments provide a partial view of the interaction phenomenon, all together permit us to advance in the comprehension of the complex interactions that may take place at the cell surface. Models, as those studied herein, provide advances in the understanding of their interactions taking into account also their presentation as glycoconjugates within a dynamic membrane-based assembly.

We demonstrated this by specifically investigating the interactions of homo- and heteromultivalent lactose-bearing glycomacromolecules with two different galectin receptors. NMR provided a specific perspective on the interaction as well-defined molecular systems (the single macromolecules or monovalent lectins) were employed. The presence of bivalent lectins and the existence of cross linking provides the impetus for the formation of large complexes that are invisible to the NMR but were detected through cryo-EM. Molecular modeling then provides additional hints for the ligand−receptor encounters, which initially follow the recognition features that take place using the individual lectin and sugar systems but then move toward multivalent interactions.

These models obviously afford a simplified view of the actual phenomenon taking place at the cell surface but highlight the fact that the galectins can effectively recognize the lactose molecules that are decorating the glycomacromolecules and that hGal1 can make simultaneous interactions with two lactose moieties present at two different glycomacromolecules, either within the same liposome (as in the model) or at different ones. According to the molecular models, simultaneous interactions with hGal3 monomers, although probably with an important entropy cost, within the same glycomacromolecule may also take place, but crosslinking cannot be envisaged. Indeed, as demonstrated by the NMR-based competition experiments, this interaction process is reversible and can be driven backward almost completely in the presence of an excess of lactose. In contrast, when bivalent hGal1 is employed and crosslinking takes place, the formed supramolecular assemblies are extremely stable and cannot be overturned by lactose.

4. MATERIALS AND METHODS

4.1. Materials. All reagents and solvents were used without further purification. *N*-[*N*′-(Succinimidyloxy glutaryl)-aminopropylpolyoxyethyleneoxycarbonyl]-1,2-distearoyl-*sn*-*glycero*-3-phosphoethanolamine sodium salt = SUNBRIGHT DSPE-020GS (DSPE-PEG-NHS) was purchased from NOF Europe. 1-[bis(Dimethylamino)methylene]-1H-1,2,3-triazolo-[4,5-*b*]pyridinium 3-oxide hexafluorophosphate, hexafluorophosphate azabenzotriazole tetramethyl uronium (HATU) was purchased from Abcr. Anhydrous $CuSO_4$, DMSO, piperidine, sodium methoxide, and triisopropylsilane (TIPS) were purchased from Acros Organics. Sodium diethyldithiocarbamate was purchased from Alfa Aesar. DMF (for peptide synthesis) was purchased from Biosolve. DIPEA was purchased from Carl Roth. Acetonitrile, dichloromethane, and trifluoro acetic acid (TFA) were purchased from Fischer Scientific. Diethylether was purchased from Honeywell. Benzotriazol-1-yl-oxytripyrrolidinophosphonium hexafluorophosphate (PyBOP) and Boc-L-alanine-OH were purchased from Iris Biotech. 4-Amino benzene sulfonic acid was purchased from J&K. Lithium hydroxide was purchased from PanReac AppliChem. Acetic acid, methanol (MeOH), sodium ascor-

https://doi.org/10.1021/acsomega.3c00634
ACS Omega 2023, 8, 16883−16895

bate, $NaHCO_3$, tetrahydrofuran, and Boc-β-Alanine-OH were purchased from Sigma-Aldrich.

Solid-phase synthesis was performed on the TentaGel S RAM resin purchased from Rapp Polymere using polypropylene reactors equipped with polyethylene frits and closed with Luer-stoppers from MultiSyntech GmbH. Slide-A-Lyzer Dialysis Cassettes were purchased from Thermo Scientific. Anion exchange resin AG1-X8, quat. Ammonium, 100−200 mesh, as the acetate form was purchased from BioRad.

Building blocks triple bond diethylenetriamine succinyl, 1-(fluorenyl)-3,11-dioxo-7-(pent-4-ynoyl)-2-oxa-4,7,10-triazatetra-decan-14-oic acid (TDS), ethylene glycol diamine succinyl, 1-(9*H*-fluoren-9-yl)-3,14-dioxo-2,7,10-trioxa-4,13-diazaheptadecan-17-oic acid (EDS), and methyl succinyl diethylenetriamine succinyl, 1-(9*H*-fluoren-9-yl)-7-(4-methoxy-4-oxobutanoyl)-3,11-dioxo-2-oxa-4,7,10-triazatetradecan-14-oic acid (MDS) were synthesized as reported earlier.[27,32,35]

(2-Azidoethyl)-2,3,4,6-tetra-*O*-acetyl-α-D-glucopyranoside and hepta-*O*-acetyl-β-lactosylazide were synthesized following established protocols.[50]

Reactions were monitored with analytical thin-layer chromatography conducted on Merck silica gel 60 F254 plates and visualized with ninhydrin and anisaldehyde staining. ^{1}H-NMR spectra for compound characterization were measured on a Bruker AVANCE III 600. Analytical RP-HPLC measurements were performed on Agilent Technologies 6120 series coupled with an Agilent quadrupole mass spectrometer. All spectra were measured with solvents A: 95% H_2O, 5% ACN, +0.1% formic acid and solvent B: 5% H_2O, 95% ACN, +0.1% formic acid. Purities of the compounds were determined by integration of the UV-signals absorbing at 214 nm. Preparative RP-HPLC was performed on an Agilent 1200 series. High-resolution ESI (HR-ESI) spectra were measured on UHR-QTOF maXis 4G (Bruker Daltonics). Matrix-assisted laser desorption ionization-time of flight-mass spectrometry (MALDI-TOF-MS) was performed on a Bruker MALDI-TOF-MS Ultraflex I System.

4.1.1. Lipids. eggPC (L-α-phosphatidylcholine 840051) was purchased from Avanti Polar Lipids. All other materials (salts and organic solvents) were of analytical grade.

4.2. Methods. *4.2.1. Solid-Phase Synthesis.* General solid-phase synthesis was performed as reported.[27,32] The protocol is described for a batch size of 0.1 mmol. Reactions were performed in a polypropylene syringe reactor with polyethylene frits on a shaker.

4.2.2. Resin Preparation and Fmoc Cleavage. 0.1 mmol resin (400 mg with resin loading 0.25 mmol/g) was transferred into a 10 mL reactor and swollen with 5 mL of DCM for 30 min. The resin was washed ten times with DMF, and Fmoc was cleaved by the addition of 5 mL of 25% piperidine in DMF solution for 10 and again for 20 min. In between the deprotection steps, the resin was washed three times and afterward fifteen times with 5 mL of DMF each.

4.2.3. Building Block Coupling. 5 equiv (0.5 mmol) of the building block and PyBOP were dissolved in 4 mL of DMF, 20 equiv of DIPEA (2 mmol) was added, and the reaction mixture was drawn into the syringe and shaken for 1 h. Then, the resin was washed 15 times with 5 mL of DMF each.

4.2.4. Deprotection of the Carboxylic Side Chain. Before deprotection, the resin was washed five times with 5 mL of THF/H_2O (1/1). Then, the resin was treated with 5 mL of a 0.2 M LiOH-solution in THF/H_2O (1/1) twice for 1 h each. In between, the resin was washed three times with 5 mL of THF/H_2O (1/1). After the second deprotection, the resin was washed five times with water, DMF, DCM, and again DMF.

4.2.5. Side Chain Coupling. 3 equiv per carboxylic acid group of HATU was dissolved in 1.5 mL of DMF, 10 equiv of DIPEA was added, and the mixture was drawn into a syringe. For preactivation, the resin wash shaken for 15 min. Afterward, a solution of 3 equiv per carboxylic acid group of 4-amino benzene sulfonic acid in 1.5 mL of DMF was added, and the reaction was shaken for 1.5 h.

4.2.6. Copper-Catalyzed Alkyne Azide Cycloaddition. 2.5 equiv of the carbohydrate azide derivative per alkyne was dissolved in 2 mL of DMF. Separately, 50 mol % per alkyne of $CuSO_4$ and sodium ascorbate were each dissolved in 0.2 mL of MilliQ water. First, the carbohydrate solution followed by sodium ascorbate and then copper sulfate were drawn into the syringe. After reaction overnight, the resin was washed extensively with DMF, a solution of 0.2 M sodium diethyldithiocarbamate in DMF/water (1/1), water, and DCM until no more color changes were monitored.

4.2.7. Carbohydrate Deprotection. The resin was treated two times for 30 min with 5 mL of 0.2 M sodium methoxide solution in MeOH. In between, the resin was washed three times with 5 mL of MeOH. Afterward, the resin was washed five times with 5 mL of MeOH and ten times with DMF.

4.2.8. Release of the Free Terminal Amine. For the generation of a free terminal amine for structures **1** and **6**, the terminal EDS was left Fmoc-protected during the CuAAC until the end of the synthesis and only then deprotected. For structures **2** to **5**, Boc-protected alanine was used as the final building block since the basic deprotection conditions of MDS could also lead to a loss of Fmoc-protecting groups (for **2**, **3**, **5** β-alanine, for **4** α-alanine). Boc was removed under the acidic cleavage conditions during the final cleavage of the compounds.

4.2.9. Macro Cleavage. The resin was washed ten times with 5 mL of DCM. A cleavage mixture consisting of 95% TFA, 2.5% TIPS, and 2.5% DCM was added to the resin and shaken for 1 h. The mixture was added dropwise to cold diethylether for precipitation of the product. The supernatant was decanted, and the white precipitate was dried under a nitrogen stream. The resulting solid was dissolved in water for lyophilization.

4.2.10. TFA Removal. For TFA removal according to a protocol by Roux et al. for a 100 mg sample, 1000 mg of the anion exchange resin was used.[51] First, the resin was activated by washing three times with 10 mL of a 1.6 M acetic acid solution and three times with 10 mL of a 0.16 M acetic acid solution. The sample was dissolved in 10 mL of water and added to the resin. The syringe was shaken for 1 h. Then, the supernatant was collected and the resin washed three times with 2 mL of water each. The aqueous phase was lyophilized to obtain the crude product. Subsequently, products were purified via preparative RP-HPLC to obtain the products as a white solid with purities above 95%.

4.2.11. Lipid Conjugation.[37] For **L1** and **L6**, DSPE-PEG-NHS (12 mg, 1 equiv) was dissolved in 600 μL of DMF and mixed with a solution of 8 equiv of **1** and **6**, respectively, dissolved in 5.4 mL of 0.1 M $NaHCO_3$ buffer (pH = 8.4). The mixture was stirred overnight. After removal of the solvents under reduced pressure, the compound was redissolved in 0.1 M $NaHCO_3$-buffer and dialyzed with Slide-A-Lyzer cassettes (MWCO = 7000 g/mol) three times for 8−12 h against the

https://doi.org/10.1021/acsomega.3c00634
ACS Omega 2023, 8, 16883−16895

buffer and three times for 8−12 h against water with a sample to solvent ratio of 1 to 250−550 mL.

For **L2** to **L5**, DSPE-PEG-NHS (1 equiv) and glycomacromolecules **2**−**5** (5 equiv) were dissolved in DMSO (0.5 mL per 1 mg lipid), 20 equiv of DIPEA was added, and the mixture was stirred overnight. The solvent was removed under reduced pressure and the residuals were redissolved in water and dialyzed four times for 8−12 h against water with Slide-A-Lyzer cassettes (MWCO = 7000 g/mol).

All samples were obtained after lyophilization as white solids. Yields given in milligrams relate to the successfully conjugated lipids. The content of unconjugated lipids was quantified via ^{1}H-NMR and excluded in the calculation.

4.2.12. Protein Expression and Purification. Galectins' (hGal3-CRD and hGal1) expression and purification are described elsewhere.[30,43] Briefly, for the labeled protein, a 5 mL overnight culture was added in 1 L of M9 media containing the antibiotic and ^{15}N−NH_4Cl (1 g) as the nitrogen source. When the OD_{600} value was between 0.7−1.2, protein expression was induced by addition of 1 mM isopropyl β-D-1-thio-galactopyranoside (IPTG) and growth continued for 3 h at 37 °C. Afterward, cells were harvested and resuspended in column buffer (PBS 1× pH 7.2, 2 mM EDTA, 2 mM β-mercarptoethanol/DTT, 0.1% NaN_3), and 1 mM PMSF was added to inhibit protease cleavage. The suspension was sonicated and the crude extract clarified by centrifugation at 35000 rpm for 30 min at 4 °C. The soluble fraction was loaded onto a pre-equilibrated α-Lactose-Agarose resin (Sigma-Aldrich) column and washed with 50 mL of column buffer. To elute recombinant proteins, 7 mL of elution buffer (150 mM α-Lactose in column buffer) was injected. Protein purity was checked by SDS-PAGE and subsequently confirmed by LC−MS.

Both galectins were thoroughly dialyzed against PBS, pH 7.4, until no lactose was present, before use.

4.2.13. Liposome Preparation. Powdered phosphatidylcholine and conjugated glycomacromolecules were dissolved in an organic solution (2:1 chloroform/methanol, v/v). The desired amount was transferred to a glass vial, evaporated to dryness under a N_2 stream, and kept under vacuum for 2 h in order to remove all the organic solvent. The obtained lipid film was then hydrated with the desired buffer (PBS pH 7.4) and vigorously vortexed to obtain multilamellar vesicles. Afterward, the samples were subjected to 10 freeze and thaw cycles and extruded through 0.1 μM pore-size Nucleopore filters using a mini-extruder. LUVs of 100 nm diameter were obtained.

4.2.14. NMR Experiments. All spectra were performed at 298 K on a Bruker AVANCE 2600 MHz spectrometer.

The ^{1}H NMR resonances of the ligands were assigned through total correlation spectroscopy (60 and 90 ms mixing times), nuclear Overhauser enhancement spectroscopy (500 or 600 ms mixing times), and HSQC experiments using a Bruker AVANCE 2600 MHz spectrometer equipped with a standard triple-channel probe (600 MHz). Ligands were dissolved in deuterated phosphate buffered saline solutions at a concentration of 1 mM.

For STD experiments, 40 μM of full-length hGal3 or hGal1 was prepared in deuterated PBS and around 70 equiv of the ligand was added. The on-resonance frequency was set at the aliphatic region (~0.77 ppm) and the off-resonance frequency at −25 ppm. To achieve protein saturation, a series of 25−50 ms PC9 pulses was used with a total saturation time of the protein of 2 s in a 600 MHz spectrometer. A spin-lock filter (10 ms) was used to remove the NMR signals of the macromolecule.

To analyze the binding of the glycomacromolecules in liposomes to galectins, ^{1}H−^{15}N HSQC readings were recorded on 50 μM ^{15}N-hGal3-CRD and ^{15}N-hGal1, at 298 K on a Bruker AVANCE 2600 MHz equipped with a standard triple-channel probe. CSP and crosspeak volume were followed using CcpNmr Analysis 2.4.2 software.[52]

4.2.15. Cryo-EM Sample Preparation and Data Collection. Liposomes containing **L1** glycomacromolecules and galectins were vitrified onto previously glow-discharged Quantifoil R2/2 copper grids 300 mesh using the automatic plunge freezer EM GP2 (Leica). For each sample, 4 μL was loaded onto the grid and after 20 s of incubation, a 1.8 s blotting was performed. The vitrified grids corresponding to the different samples were visualized using the in-house 200 kV field emission gun JEM-2200 FS (JEOL) transmission electron microscope quipped with a K2 direct detector camera (GATAN). The cryo-images were collected in linear mode at defocus values ranging from −2 to −2.5 μM, with a total dose of about 50 e^{-}/Å^2 and a pixel size of 2 Å at the specimen.

4.3. Computational Methods. *4.3.1. Model Building.* A 422 unit POPC bilayer (approximately 120 Å by 120 Å) was generated using the CHARMM-GUI[53] membrane builder. A single glycolipid for the hGal3 simulation and two glycolipids for the hGal1 simulation were manually embedded into the membrane. This corresponds to the 29.8:0.2 mM ratio between PC and Lac(1,3,5)-6-PEG-DSPE used in the experimental formulation of the liposomes. Glycolipids are composed of 1,2-distearoyl-*sn*-glycero-3-phosphoethanolamine-poly(ethylene glycol) (DSPE-PEG), a common phospholipid−polymer conjugate in drug delivery applications,[54] which are functionalized with three lactose units (Lac(1,3,5)-6-PEG-DSPE). The PEG linker is 44 units long, providing a separation of approximately 200 Å between the lactose groups and the membrane. Galectins were docked onto the lactose groups. Initial coordinates for hGal3 and hGal1 were generated from reported crystallographic structures (PDB ID 4R9C and 1W6O, respectively).[48,49] An example of an extended model used as a starting geometry for molecular dynamics (MD) simulations is represented in Figure S6.

4.3.2. MD Simulations. All-atom MD simulations were carried out with AMBER 20[55] using the ff14SB[56] force field for proteins, GLYCAM 06j-1[57] for glycans, Lipid14[58] for lipids and gaff2[59] for the linkers, and using periodic boundary conditions. Membrane-glycolipid-galectin models were immersed in a water box of TIP3P[60] water molecules and neutralized by adding explicit Na^{+}/Cl^{-} counterions. The system was subjected to 5000 steepest descent and 5000 conjugate gradient geometry optimization steps and then heated from 0 to 300 K along a 100 ps simulation in the *NVT* ensemble using the Langevin thermostat.[61] This was followed by a 1 ns MD simulation in the *NPT* ensemble to adjust the water density. In both simulations, a harmonic constraint of 10 kcal mol^{-1} Å^{-2} was enforced onto all atoms except water and counterions. In a further step, restraints on the lipid bilayer were removed while keeping the protein and glycolipid restrained. Finally, all constraints were removed to allow the system to fully equilibrate for 1 ns. Production simulations were run for 100 ns in the NPT ensemble using anisotropic scaling and the Berendsen barostat.[62] The SHAKE[63] algorithm was employed for production with a 2 fs time step. Long-range electrostatic effects were modeled using the particle mesh

https://doi.org/10.1021/acsomega.3c00634
ACS Omega 2023, 8, 16883−16895

Ewald method, setting the width of the nonbonded "skin" at 5.0 Å in combination with a cutoff for nonbonded interactions of 10 Å. This option defines the members of the nonbonded list in particle mesh Ewald calculations and is needed to prevent code halting when membrane simulations boxes change their size and density too much along equilibration.[64] Trajectory analysis was performed using the *cpptraj* tool in AMBER.[65]

■ ASSOCIATED CONTENT

Supporting Information

The Supporting Information is available free of charge at https://pubs.acs.org/doi/10.1021/acsomega.3c00634.

Information on the synthesis and analytical data of the glycomacromolecules, MS and NMR spectra, and MD analysis (PDF)

■ AUTHOR INFORMATION

Corresponding Authors

Laura Hartmann − *Department of Organic and Macromolecular Chemistry, Heinrich-Heine-University Düsseldorf, Düsseldorf 40225, Germany;* Present Address: Institute for Macromolecular Chemistry, University of Freiburg, Stefan-Meier-Str. 31, Freiburg i.Br. 79104, Germany; orcid.org/0000-0003-0115-6405; Email: laura.hartmann@hhu.de

Jesús Jiménez-Barbero − *CIC bioGUNE, Basque Research & Technology Alliance (BRTA), Derio 48160 Bizkaia, Spain; Ikerbasque, Basque Foundation for Science, Bilbao 48009 Bizkaia, Spain; Department of Organic and Inorganic Chemistry, Faculty of Science and Technology, University of the Basque Country, EHU-UPV, 48940 Leioa, Spain; Centro de Investigación Biomédica En Red de Enfermedades Respiratorias, Madrid 28029, Spain;* orcid.org/0000-0001-5421-8513; Email: jjbarbero@cicbiogune.es

Authors

Marta G. Lete − *CIC bioGUNE, Basque Research & Technology Alliance (BRTA), Derio 48160 Bizkaia, Spain;* orcid.org/0000-0002-9654-7881

Miriam Hoffmann − *Department of Organic and Macromolecular Chemistry, Heinrich-Heine-University Düsseldorf, Düsseldorf 40225, Germany;* orcid.org/0000-0001-7709-5886

Nils Schomann − *Department of Organic and Macromolecular Chemistry, Heinrich-Heine-University Düsseldorf, Düsseldorf 40225, Germany*

Ane Martínez-Castillo − *CIC bioGUNE, Basque Research & Technology Alliance (BRTA), Derio 48160 Bizkaia, Spain*

Francesca Peccati − *CIC bioGUNE, Basque Research & Technology Alliance (BRTA), Derio 48160 Bizkaia, Spain*

Patrick B. Konietzny − *Department of Organic and Macromolecular Chemistry, Heinrich-Heine-University Düsseldorf, Düsseldorf 40225, Germany*

Sandra Delgado − *CIC bioGUNE, Basque Research & Technology Alliance (BRTA), Derio 48160 Bizkaia, Spain*

Nicole L. Snyder − *Department of Chemistry, Davidson College, Davidson, North Carolina 28035, United States;* orcid.org/0000-0002-2508-4090

Gonzalo Jiménez-Oses − *CIC bioGUNE, Basque Research & Technology Alliance (BRTA), Derio 48160 Bizkaia, Spain; Ikerbasque, Basque Foundation for Science, Bilbao 48009 Bizkaia, Spain;* orcid.org/0000-0003-0105-4337

Nicola G. A. Abrescia − *CIC bioGUNE, Basque Research & Technology Alliance (BRTA), Derio 48160 Bizkaia, Spain; Ikerbasque, Basque Foundation for Science, Bilbao 48009 Bizkaia, Spain; Centro de Investigación Biomédica en Red de Enfermedades Hepáticas y Digestivas, Instituto de Salud Carlos III, Madrid 28029, Spain;* orcid.org/0000-0001-5559-1918

Ana Ardá − *CIC bioGUNE, Basque Research & Technology Alliance (BRTA), Derio 48160 Bizkaia, Spain; Ikerbasque, Basque Foundation for Science, Bilbao 48009 Bizkaia, Spain;* orcid.org/0000-0003-3027-7417

Complete contact information is available at: https://pubs.acs.org/10.1021/acsomega.3c00634

Author Contributions

[▽]M.G.L. and M.H. authors have contributed equally.

Notes

The authors declare no competing financial interest.

■ ACKNOWLEDGMENTS

M.H. and L.H. thank the DFG for support through the ViroCarb research consortium (HA5950/5-2) and the CeMSA@HHU (Center for Molecular and Structural Analytics @ Heinrich-Heine University) for recording the mass spectrometric and the NMR-spectroscopic data for the structural conformation of the glycomacromolecules and their lipid conjugates. The CIC bioGUNE EM platform is also thanked for infrastructural support during cryo-EM data collection. The group in Spain thank the European Research Council (RECGLYCANMR, Advanced grant no. 788143), MCIN/AEI/10.13039/501100011033 for grants PDI2021-1237810B-C21, PID2021-126130OB-I00, CEX2021-001136-S, and CIBERES, an initiative of Instituto de Salud Carlos III (ISCIII), Madrid, Spain, for generous funding.

■ REFERENCES

(1) Vasta, G. R. Galectins in Host-Pathogen Interactions: Structural, Functional and Evolutionary Aspects. *Adv. Exp. Med. Biol.* **2020**, *1204*, 169−196.

(2) Taylor, M. E.; Drickamer, K. Mammalian sugar-binding receptors: known functions and unexplored roles. *FEBS J.* **2019**, *286*, 1800−1814.

(3) Zheng, Y.; Feng, W.; Wang, Y. J.; Sun, Y.; Shi, G.; Yu, Q. Galectins as potential emerging key targets in different types of leukemia. *Eur. J. Pharmacol.* **2019**, *844*, 73−78.

(4) Blanda, V.; Bracale, U. M.; Di Taranto, M. D.; Fortunato, G. Galectin-3 in Cardiovascular Diseases. *Int. J. Mol. Sci.* **2020**, *21*, 9232.

(5) Vasta, G. R. Roles of galectins in infection. *Nat. Rev. Microbiol.* **2009**, *7*, 424−438.

(6) Rabinovich, G. A.; Gruppi, A. Galectins as immunoregulators during infectious processes: from microbial invasion to the resolution of the disease. *Parasite Immunol.* **2005**, *27*, 103−114.

(7) Paulson, J. C.; Blixt, O.; Collins, B. E. Sweet spots in functional glycomics. *Nat. Chem. Biol.* **2006**, *2*, 238−248.

(8) *Essentials of Glycobiology*; Varki, A.; Cummings, R. D.; Esko, J. D.; Stanley, P.; Hart, G. W.; Aebi, M.; Darvill, A. G.; Kinoshita, T.; Packer, N. H.; Prestegard, J. H.; Schnaar, R. L.; Seeberger, P. H., Eds. Cold Spring Harbor: (NY), 2015, rd.

(9) Grant, O. C.; Smith, H. M.; Firsova, D.; Fadda, E.; Woods, R. J. Presentation, presentation, presentation! Molecular-level insight into linker effects on glycan array screening data. *Glycobiology* **2014**, *24*, 17−25.

(10) Gimeno, A.; Reichardt, N. C.; Canada, F. J.; Perkams, L.; Unverzagt, C.; Jimenez-Barbero, J.; Arda, A. NMR and Molecular Recognition of N-Glycans: Remote Modifications of the Saccharide Chain Modulate Binding Features. *ACS Chem. Biol.* **2017**, *12*, 1104−1112.
(11) Critcher, M.; O'Leary, T.; Huang, M. L. Glycoengineering: scratching the surface. *Biochem. J.* **2021**, *478*, 703−719.
(12) Honigfort, D. J.; Altman, M. O.; Gagneux, P.; Godula, K. Glycocalyx crowding with mucin mimetics strengthens binding of soluble and virus-associated lectins to host cell glycan receptors. *Proc. Natl. Acad. Sci. U.S.A.* **2021**, *118*, No. e2107896118.
(13) Johannes, L.; Jacob, R.; Leffler, H. Galectins at a glance. *J. Cell Sci.* **2018**, *131*, jcs208884.
(14) Laaf, D.; Bojarová, P.; Elling, L.; Křen, V. Galectin−Carbohydrate Interactions in Biomedicine and Biotechnology. *Trends Biotechnol.* **2019**, *37*, 402−415.
(15) Tavares, M. R.; Blahova, M.; Sedlakova, L.; Elling, L.; Pelantova, H.; Konefal, R.; Etrych, T.; Kren, V.; Bojarova, P.; Chytil, P. High-Affinity N-(2-Hydroxypropyl)methacrylamide Copolymers with Tailored N-Acetyllactosamine Presentation Discriminate between Galectins. *Biomacromolecules* **2020**, *21*, 641−652.
(16) Mauris, J.; Mantelli, F.; Woodward, A. M.; Cao, Z.; Bertozzi, C. R.; Panjwani, N.; Godula, K.; Argueso, P. Modulation of ocular surface glycocalyx barrier function by a galectin-3 N-terminal deletion mutant and membrane-anchored synthetic glycopolymers. *PLoS One* **2013**, *8*, No. e72304.
(17) Tang, J. S. J.; Rosencrantz, S.; Tepper, L.; Chea, S.; Klopzig, S.; Kruger-Genge, A.; Storsberg, J.; Rosencrantz, R. R. Functional Glyco-Nanogels for Multivalent Interaction with Lectins. *Molecules* **2019**, *24*, 1865.
(18) Zhang, H.; Laaf, D.; Elling, L.; Pieters, R. J. Thiodigalactoside-Bovine Serum Albumin Conjugates as High-Potency Inhibitors of Galectin-3: An Outstanding Example of Multivalent Presentation of Small Molecule Inhibitors. *Bioconjugate Chem.* **2018**, *29*, 1266−1275.
(19) Soomro, Z. H.; Cecioni, S.; Blanchard, H.; Praly, J. P.; Imberty, A.; Vidal, S.; Matthews, S. E. CuAAC synthesis of resorcin[4]arene-based glycoclusters as multivalent ligands of lectins. *Org. Biomol. Chem.* **2011**, *9*, 6587−6597.
(20) Heine, V.; Hovorkova, M.; Vlachova, M.; Filipova, M.; Bumba, L.; Janouskova, O.; Hubalek, M.; Cvacka, J.; Petraskova, L.; Pelantova, H.; Kren, V.; Elling, L.; Bojarova, P. Immunoprotective neoglycoproteins: Chemoenzymatic synthesis of multivalent glycomimetics for inhibition of cancer-related galectin-3. *Eur. J. Med. Chem.* **2021**, *220*, 113500.
(21) Lepur, A.; Salomonsson, E.; Nilsson, U. J.; Leffler, H. Ligand induced galectin-3 protein self-association. *J. Biol. Chem.* **2012**, *287*, 21751−21756.
(22) Bojarova, P.; Kren, V. Sugared biomaterial binding lectins: achievements and perspectives. *Biomater. Sci.* **2016**, *4*, 1142−1160.
(23) Dam, T. K.; Brewer, F. C. Maintenance of cell surface glycan density by lectin-glycan interactions: a homeostatic and innate immune regulatory mechanism. *Glycobiology* **2010**, *20*, 1061−1064.
(24) Wisnovsky, S.; Bertozzi, C. R. Reading the glyco-code: New approaches to studying protein-carbohydrate interactions. *Curr. Opin. Struct. Biol.* **2022**, *75*, 102395.
(25) Lete, M. G.; Franconetti, A.; Delgado, S.; Jimenez-Barbero, J.; Arda, A. Oligosaccharide Presentation Modulates the Molecular Recognition of Glycolipids by Galectins on Membrane Surfaces. *Pharmaceuticals* **2022**, *15*, 145.
(26) Vance, J. A.; Devaraj, N. K. Membrane Mimetic Chemistry in Artificial Cells. *J. Am. Chem. Soc.* **2021**, *143*, 8223−8231.
(27) Freichel, T.; Heine, V.; Laaf, D.; Mackintosh, E. E.; Sarafova, S.; Elling, L.; Snyder, N. L.; Hartmann, L. Sequence-Defined Heteromultivalent Precision Glycomacromolecules Bearing Sulfonated/Sulfated Nonglycosidic Moieties Preferentially Bind Galectin-3 and Delay Wound Healing of a Galectin-3 Positive Tumor Cell Line in an In Vitro Wound Scratch Assay. *Macromol. Biosci.* **2020**, *20*, 2000163.
(28) Freichel, T.; Laaf, D.; Hoffmann, M.; Konietzny, P. B.; Heine, V.; Wawrzinek, R.; Rademacher, C.; Snyder, N. L.; Elling, L.; Hartmann, L. Effects of linker and liposome anchoring on lactose-functionalized glycomacromolecules as multivalent ligands for binding galectin-3. *RSC Adv.* **2019**, *9*, 23484−23497.
(29) Arda, A.; Jimenez-Barbero, J. The recognition of glycans by protein receptors. Insights from NMR spectroscopy. *Chem. Commun.* **2018**, *54*, 4761−4769.
(30) Bertuzzi, S.; Gimeno, A.; Nunez-Franco, R.; Bernardo-Seisdedos, G.; Delgado, S.; Jimenez-Oses, G.; Millet, O.; Jimenez-Barbero, J.; Arda, A. Unravelling the Time Scale of Conformational Plasticity and Allostery in Glycan Recognition by Human Galectin-1. *Chemistry* **2020**, *26*, 15643−15653.
(31) Bertuzzi, S.; Quintana, J. I.; Arda, A.; Gimeno, A.; Jimenez-Barbero, J. Targeting Galectins With Glycomimetics. *Front. Chem.* **2020**, *8*, 593.
(32) Ponader, D.; Wojcik, F.; Beceren-Braun, F.; Dernedde, J.; Hartmann, L. Sequence-defined glycopolymer segments presenting mannose: synthesis and lectin binding affinity. *Biomacromolecules* **2012**, *13*, 1845−1852.
(33) Baier, M.; Giesler, M.; Hartmann, L. Split-and-Combine Approach Towards Branched Precision Glycomacromolecules and Their Lectin Binding Behavior. *Chemistry* **2018**, *24*, 1619−1630.
(34) Boden, S.; Wagner, K. G.; Karg, M.; Hartmann, L. Presenting Precision Glycomacromolecules on Gold Nanoparticles for Increased Lectin Binding. *Polymers* **2017**, *9*, 716.
(35) Ebbesen, M. F.; Gerke, C.; Hartwig, P.; Hartmann, L. Biodegradable Poly(amidoamine)s with Uniform Degradation Fragments via Sequence-Controlled Macromonomers. *Polym. Chem.* **2016**, *7*, 7086−7093.
(36) Zemplén, G.; Pacsu, E. Über die Verseifung acetylierter Zucker und verwandter Substanzen. *Ber. Dtsch. Chem. Ges. A and B* **2006**, *62*, 1613−1614.
(37) Wamhoff, E. C.; Schulze, J.; Bellmann, L.; Rentzsch, M.; Bachem, G.; Fuchsberger, F. F.; Rademacher, J.; Hermann, M.; Del Frari, B.; van Dalen, R.; Hartmann, D.; van Sorge, N. M.; Seitz, O.; Stoitzner, P.; Rademacher, C. A Specific, Glycomimetic Langerin Ligand for Human Langerhans Cell Targeting. *ACS Cent. Sci.* **2019**, *5*, 808−820.
(38) Lim, C. Y.; Owens, N. A.; Wampler, R. D.; Ying, Y.; Granger, J. H.; Porter, M. D.; Takahashi, M.; Shimazu, K. Succinimidyl Ester Surface Chemistry: Implications of the Competition between Aminolysis and Hydrolysis on Covalent Protein Immobilization. *Langmuir* **2014**, *30*, 12868−12878.
(39) Miller, M. C.; Nesmelova, I. V.; Platt, D.; Klyosov, A.; Mayo, K. H. The carbohydrate-binding domain on galectin-1 is more extensive for a complex glycan than for simple saccharides: implications for galectin-glycan interactions at the cell surface. *Biochem. J.* **2009**, *421*, 211−221.
(40) Dings, R. P. M.; Miller, M. C.; Griffin, R. J.; Mayo, K. H. Galectins as Molecular Targets for Therapeutic Intervention. *Int. J. Mol. Sci.* **2018**, *19*, 905.
(41) Mayer, M.; Meyer, B. Characterization of Ligand Binding by Saturation Transfer Difference NMR Spectroscopy. *Angew. Chem., Int. Ed. Engl.* **1999**, *38*, 1784−1788.
(42) Meyer, B.; Peters, T. NMR spectroscopy techniques for screening and identifying ligand binding to protein receptors. *Angew. Chem., Int. Ed. Engl.* **2003**, *42*, 864−890.
(43) Gimeno, A.; Delgado, S.; Valverde, P.; Bertuzzi, S.; Berbis, M. A.; Echavarren, J.; Lacetera, A.; Martin-Santamaria, S.; Surolia, A.; Canada, F. J.; Jimenez-Barbero, J.; Arda, A. Minimizing the Entropy Penalty for Ligand Binding: Lessons from the Molecular Recognition of the Histo Blood-Group Antigens by Human Galectin-3. *Angew. Chem., Int. Ed. Engl.* **2019**, *58*, 7268−7272.
(44) van Heteren, J.; Pieters, R. J. Chapter Nine - Carbohydrate-protein interactions: Enhancing multivalency effects through statistical rebinding. In *Carbohydrates in Drug Discovery and Development*; Tiwari, V. K., Ed.; Elsevier, 2020; pp 383−402.

https://doi.org/10.1021/acsomega.3c00634
ACS Omega 2023, 8, 16883−16895

(45) Newberry, R. W.; Raines, R. T. Secondary Forces in Protein Folding. *ACS Chem. Biol.* **2019**, *14*, 1677−1686.
(46) Boden, S.; Reise, F.; Kania, J.; Lindhorst, T. K.; Hartmann, L. Sequence-Defined Introduction of Hydrophobic Motifs and Effects in Lectin Binding of Precision Glycomacromolecules. *Macromol. Biosci.* **2019**, *19*, 1800425.
(47) Bertuzzi, S.; Gimeno, A.; Martinez-Castillo, A.; Lete, M. G.; Delgado, S.; Airoldi, C.; Rodrigues Tavares, M.; Blahova, M.; Chytil, P.; Kren, V.; Abrescia, N. G. A.; Arda, A.; Bojarova, P.; Jimenez-Barbero, J. Cross-Linking Effects Dictate the Preference of Galectins to Bind LacNAc-Decorated HPMA Copolymers. *Int. J. Mol. Sci.* **2021**, *22*, 6000.
(48) Su, J.; Zhang, T.; Wang, P.; Liu, F.; Tai, G.; Zhou, Y. The water network in galectin-3 ligand binding site guides inhibitor design. *Acta Biochim. Biophys. Sin.* **2015**, *47*, 192−198.
(49) López-Lucendo, M. F.; Solís, D.; André, S.; Hirabayashi, J.; Kasai, K.; Kaltner, H.; Gabius, H. J.; Romero, A. Growth-regulatory human galectin-1: crystallographic characterisation of the structural changes induced by single-site mutations and their impact on the thermodynamics of ligand binding. *J. Mol. Biol.* **2004**, *343*, 957−970.
(50) Wu, L.; Sampson, N. S. Fucose, mannose, and beta-N-acetylglucosamine glycopolymers initiate the mouse sperm acrosome reaction through convergent signaling pathways. *ACS Chem. Biol.* **2014**, *9*, 468−475.
(51) Roux, S.; Zekri, E.; Rousseau, B.; Paternostre, M.; Cintrat, J. C.; Fay, N. Elimination and exchange of trifluoroacetate counter-ion from cationic peptides: a critical evaluation of different approaches. *J. Pept. Sci.* **2008**, *14*, 354−359.
(52) Vranken, W. F.; Boucher, W.; Stevens, T. J.; Fogh, R. H.; Pajon, A.; Llinas, M.; Ulrich, E. L.; Markley, J. L.; Ionides, J.; Laue, E. D. The CCPN data model for NMR spectroscopy: development of a software pipeline. *Proteins* **2005**, *59*, 687−696.
(53) Jo, S.; Kim, T.; Iyer, V. G.; Im, W. CHARMM-GUI: a web-based graphical user interface for CHARMM. *J. Comput. Chem.* **2008**, *29*, 1859−1865.
(54) Che, J.; Okeke, C. I.; Hu, Z. B.; Xu, J. DSPE-PEG: a distinctive component in drug delivery system. *Curr. Pharm. Des.* **2015**, *21*, 1598−1605.
(55) Case, D. A.; Belfon, K.; Ben-Shalom, I. Y.; Brozell, S. R.; Cerutti, D. S.; Cheatham, T. E., III; Cruzeiro, V. W. D.; Darden, T. A.; Duke, R. E.; Giambasu, G.; Gilson, M. K.; Gohlke, H.; Goetz, A. W.; Harris, R.; Izadi, S.; Izmailov, S. A.; Kasavajhala, K.; Kovalenko, A.; Krasny, R.; Kurtzman, T.; Lee, T. S.; LeGrand, S.; Li, P.; Lin, C.; Liu, J.; Luchko, T.; Luo, R.; Man, V.; Merz, K. M.; Miao, Y.; Mikhailovskii, O.; Monard, G.; Nguyen, H.; Onufriev, A.; Pan, F.; Pantano, S.; Qi, R.; Roe, D. R.; Roitberg, A.; Sagui, C.; Schott-Verdugo, S.; Shen, J.; Simmerling, C.; Skrynnikov, N. R.; Smith, J.; Swails, J.; Walker, R. C.; Wang, J.; Wilson, L.; Wolf, R. M.; Wu, X.; Xiong, Y.; Xue, Y.; York, D. M.; Kollman, P. A. *AMBER 2020*; University of California, 2020.
(56) Maier, J. A.; Martinez, C.; Kasavajhala, K.; Wickstrom, L.; Hauser, K. E.; Simmerling, C. ff14SB: Improving the Accuracy of Protein Side Chain and Backbone Parameters from ff99SB. *J. Chem. Theory Comput.* **2015**, *11*, 3696−3713.
(57) Kirschner, K. N.; Yongye, A. B.; Tschampel, S. M.; Gonzalez-Outeirino, J.; Daniels, C. R.; Foley, B. L.; Woods, R. J. GLYCAM06: a generalizable biomolecular force field. Carbohydrates. *J. Comput. Chem.* **2008**, *29*, 622−655.
(58) Dickson, C. J.; Madej, B. D.; Skjevik, A. A.; Betz, R. M.; Teigen, K.; Gould, I. R.; Walker, R. C. Lipid14: The Amber Lipid Force Field. *J. Chem. Theory Comput.* **2014**, *10*, 865−879.
(59) Wang, J.; Wolf, R. M.; Caldwell, J. W.; Kollman, P. A.; Case, D. A. Development and testing of a general amber force field. *J. Comput. Chem.* **2004**, *25*, 1157−1174.
(60) Jorgensen, W. L.; Chandrasekhar, J.; Madura, J. D.; Impey, R. W.; Klein, M. L. Comparison of simple potential functions for simulating liquid water. *J. Chem. Phys.* **1983**, *79*, 926−935.
(61) Loncharich, R. J.; Brooks, B. R.; Pastor, R. W. Langevin dynamics of peptides: the frictional dependence of isomerization rates of N-acetylalanyl-N'-methylamide. *Biopolymers* **1992**, *32*, 523−535.
(62) Berendsen, H. J. C.; Postma, J. P. M.; van Gunsteren, W. F.; DiNola, A.; Haak, J. R. Molecular dynamics with coupling to an external bath. *J. Chem. Phys.* **1984**, *81*, 3684−3690.
(63) Miyamoto, S.; Kollman, P. A. Settle: An analytical version of the SHAKE and RATTLE algorithm for rigid water models. *J. Comput. Chem.* **1992**, *13*, 952−962.
(64) Darden, T.; York, D.; Pedersen, L. Particle mesh Ewald: AnN-log(N) method for Ewald sums in large systems. *J. Chem. Phys.* **1993**, *98*, 10089−10092.
(65) Roe, D. R.; Cheatham, T. E. PTRAJ and CPPTRAJ: Software for Processing and Analysis of Molecular Dynamics Trajectory Data. *J. Chem. Theory Comput.* **2013**, *9*, 3084−3095.

https://doi.org/10.1021/acsomega.3c00634
ACS Omega 2023, 8, 16883−16895